HOKKAIDO UNIVERSITY

Title	Impact of basalt application on soil chemical properties and elemental uptake by paddy rice through enhanced rock weathering
Author(s)	Uchibayashi, Hiroshi; Maruyama, Hayato; Watanabe, Toshihiro et al.
Citation	Soil science and plant nutrition, 71(4), 484-495 https://doi.org/10.1080/00380768.2024.2448457
Issue Date	2025-01-07
Doc URL	https://hdl.handle.net/2115/97378
Rights	This is an Accepted Manuscript of an article published by Taylor & Francis in Soil science and plant nutrition on 07 Jan 2025, available at: https://doi.org/10.1080/00380768.2024.2448457.
Type	journal article
File Information	Soil Science and Plant Nutrition2024.2448457.pdf

Hokkaido University Collection of Scholarly and Academic Papers : HUSCAP

Impact of basalt application on soil chemical properties and elemental uptake by paddy rice through enhanced rock weathering

Authors: Hiroshi Uchibayashi[1], Hayato Maruyama[2], Toshihiro Watanabe[2], Shoichiro Hamamoto[2], Yo Toma[2], Atsushi Nakao[3], Kohei Kurokawa[3], Takuro Shinano[2]

Affiliation:

[1]Graduate School of Agriculture, Hokkaido University, Sapporo, Hokkaido, 060-8589, Japan

[2]Research Faculty of Agriculture, Hokkaido University, Sapporo, Hokkaido, 060-8589, Japan

[3]Graduate School of Life and Environmental Sciences, Kyoto Prefectural University, Shimogamo Hangi-cho 1-5, Sakyo, Kyoto, 606-8522, Japan

Corresponding author: Takuro Shinano, E-mail address: shinano@agr.hokudai.ac.jp, Postal address: Laboratory of Plant Nutrition, Research Faculty of Agriculture, Hokkaido University, Sapporo, Hokkaido, 060-8589, Japan, Tel: 011-706-4170

Type of contribution: original articles, full-length paper

Division of the manuscript: 8. environment

Short running title: Enhanced weathering of basalt in paddy field

Abstract

Enhanced Rock Weathering (ERW) is a negative emission technology in which crushed rock powder is applied to cropland to sequestrate carbon by enhancing chemical weathering of silicate minerals. It is a co-benefit approach to promote crop growth by supplying elements (silicon (Si), calcium (Ca), magnesium (Mg), etc.) from weathering rock as well. In this study, we cultivated paddy rice for 99 days in a pot experiment with Gray Lowland soil (pH = 6.19) with six application rates of basalt equivalent to 0, 5, 10, 20, 50, 100 t ha^{-1}. We investigated the change of soil chemical properties and elemental uptake in rice. Then, we calculated release of Si, Ca, Mg, potassium (K), and sodium (Na) from the basalt, and carbon balance between before planting and after harvest in the whole system including soil and plant. The application of the basalt increased total amount of soil available Si and exchangeable Mg and Na in pot as well as the uptake of Si and Na in rice ($p < 0.05$). There was no significant difference in arsenic, cadmium, chromium, cupper, and nickel concentrations in rice grain among the application rates of the basalt. The release of Si, Mg, and Na from the basalt increased corresponding to the application rate of the basalt, suggesting that the applied basalt was weathered during cultivation, though increased carbon sequestration by the basalt weathering was not detected in 99 days of this experiment. We clearly demonstrated that basalt powder got weathered and released Si, Mg and Na in paddy field condition and additional Si enhanced paddy rice growth.

Keywords: Paddy rice, basalt, enhanced weathering, silicon, carbon

1. Introduction

Climate change is an urgent issue to be addressed, and it is thought to be caused by the increase of carbon dioxide (CO_2) emission by anthropogenic activity (IPCC 2023). The 2015 Paris Agreement targeted to limit the temperature increase to 1.5°C above pre-industrial levels. However, it is hard to achieve that goal by just reducing the use of fossil fuels, and carbon dioxide removal (CDR) technology is necessary to be developed (Hansen et al. 2017).

In geological timescale, chemical weathering of silicate rock is known as one of the negative feedback systems of CO_2 level in the atmosphere. Calcium (Ca)- and magnesium (Mg)-rich silicate rock reacts with dissolved CO_2 in the form of carbonic acid to produce bicarbonate (eq. 1), which eventually is transported in groundwater and leached to ocean (Kantola et al. 2023).

$$CaMgSi_2O_6 + 4CO_2 + 2H_2O \rightarrow 2SiO_2 + Ca^{2+} + Mg^{2+} + 4HCO_3^- \quad \text{(eq. 1)}$$

Then, Ca^{2+}, Mg^{2+}, and bicarbonate ion increases the carbonate saturation state, thereby promoting carbonate precipitation temporarily in soil and finally in the ocean, leading to sequestration of CO_2 (eq. 2).

$$Ca^{2+} \text{ (or } Mg^{2+}) + 2HCO_3^- \rightarrow CaCO_3 \text{ (or } MgCO_3) + CO_2 + H_2O \quad \text{(eq.2)}$$

This weathering process is applied to one of the CDR technologies as Enhanced Rock Weathering (ERW) (Beerling et al. 2020). In ERW approach, finely crushed rocks are applied to land surface,

59 coastal area, and the open ocean. Applied rock powders will be weathered in higher rate than in
60 natural situation and contribute to carbon sequestration (Renforth and Henderson 2017).

61 In agricultural land, ERW approach also has a potential on the improvement of soil
62 fertility and crop production (Swoboda et al. 2022). For example, Ca and Mg, essential elements
63 for plant growth, are released from silicate minerals and supplied to crops as nutrients in the
64 process of weathering (Kantola et al. 2017; Andrews and Taylor 2019). Silicon (Si) is provided
65 as well and work as beneficial element for plant growth (Kelland et al. 2020). Further, the increase
66 of Ca and Mg concentrations leads to the increase in soil pH, which is beneficial in acidic soil
67 (Gillman et al. 2001). Also, Anda et al. (2015) reported the increase of cation exchange capacity
68 (CEC) by applying basalt powder in Oxisols, which is highly weathered soil. Moreover, if the
69 improvement of soil fertility enhances plant growth, that also leads to organic carbon
70 sequestration by promoting carbon fixation by photosynthesis.

71 Rice is the fourth most produced crop in the world (FAO STAT 2022) and known as a
72 typical Si accumulator. It absorbs Si up to 10 % on a dry weight basis in the shoot, leading to the
73 resistance to biotic and abiotic stresses (Ma 2004). However, available Si concentration in soil
74 has decreased in many paddy fields in Japan because repeated harvest of rice removes silicon
75 from soil (Kaneta 2019). Since silicate mineral can provide Si in the process of weathering, ERW
76 approach can possibly replenish available silicon in soil and improve productivity of paddy field

77 (Wang et al. 2024).

78 To date, mafic and ultramafic rocks including dunite, basalt and wollastonite have been
79 studied as preferable candidates for ERW due to their fast weathering and richness of Ca or Mg,
80 and impacts of their application on upland fields have been reported so far (Ten Berge et al. 2012;
81 Haque et al. 2019; Amann et al. 2020; Haque et al. 2020; Kelland et al. 2020; Kantola et al. 2023).
82 However, as far as we know, the study about ERW in paddy field, where the soil is exposed to
83 anaerobic condition, is quite limited. There is only one paper, which reports the application of 5 t
84 ha^{-1} of wollastonite ($CaSiO_3$) powder increased paddy rice yield and calcium carbonate in the soil
85 (Wang et al., 2024). However, the impact of basalt powder application on rice growth and carbon
86 sequestration in paddy field has not been evaluated yet. Basalt has larger reserves in the world
87 than wollastonite (Beerling et al. 2018), and contains Mg and sodium (Na) as well as Ca and Si.
88 While Si supply from basalt will enhance rice growth, Na supply can do harm on rice growth, and
89 it is necessary to investigate if basalt application affects rice production positively or negatively.

90 In this study, we evaluated the effect of basalt powder application on (i) the chemical
91 properties of paddy soil and elemental uptake and growth of paddy rice, (ii) the release of cation
92 from the basalt due to weathering, (iii) carbon balance in the whole system including soil and
93 plant after 99 days of paddy rice cultivation, with different application rates of basalt ranging from
94 0 to 100 t ha^{-1}.

2. Materials and Methods

2.1. Experimental setup

Experiments were conducted with replicated mesocosms (four replicates per treatment) in a greenhouse at Hokkaido University in Japan (43°04’18.2” N, 141°20’26.5” E). 1/2000a Wagner pots (30 cm height, 25.2 cm diameter) were used and water leaching was prevented with silicon plugs (Supplemental figure 1(a)). Soil was collected from an upland agricultural field in the campus (43°04’16.6” N, 141°20’24.8” E). The soil type was classified as a Gray Lowland soil (Nakamura et al. 2024) in Comprehensive Soil Classification System of Japan First Approximation (Obara et al. 2011) (Haplic Fluvisol in World reference base for soil resources (IUSS Working Group WRB 2022)). Soil texture was sandy clay loam, and its detailed information is presented in Yang et al. (2024, unpublished). pH(H_2O) was 6.19 and soil total carbon content was 27.4 g kg^{-1} soil, measured by the protocols below. Soil was air-dried and passed through a 5 mm sieve, and thoroughly mixed. An 8 kg portion of soil was then mixed with 4.0 g of ammonium sulfate, 1.5 g of potassium dihydrogen phosphate, and 0.42 g of potassium chloride, which equals to 170 kg N ha^{-1}, 69.9 kg P ha^{-1}, and 133 kg K ha^{-1}, respectively, that are doubled local fertilizer recommendations for paddy field (Hokkaido Research Organization 2020). Crushed basalt, described below, was mixed thoroughly with soil in 6 different application rates, which were 0, 25, 50, 100, 250, and 500 g per pot (equivalent to 0, 0.31, 0.63, 1.25, 3.13, 6.25

wt.% or 0, 5, 10, 20, 50, 100 t ha^{-1}, hereafter B0, B5, B10, B20, B50, B100), respectively. A small portion of soil was collected at this stage before planting for chemical analysis from each pot and composited in each basalt application rate treatment. The pot was filled with soil and flooded with tap water on June 13, 2022. Rice seed was sown in plastic trays on April 22 and grown in a greenhouse. Three individuals of 54-days-old seedlings of paddy rice (*Oryza sativa* L. cv. Nanatsuboshi) were transplanted in the flooded pot on June 15. The pot was flooded until ripening stage (August 26) and watered to prevent soil from completely dried until harvest. Air temperature started to be hourly measured from June 17 (Ondotori TR-52i, T&D Corporation, Nagano, Japan). The mean daily air temperature during this experiment was between 15.0 ℃ and 27.4 ℃. Rice was harvested at physiological maturity and soil was collected after harvest (September 22). After investigation of yield-related indices (i.e. panicle number, grain number, 1000 grain weight and setting rate), plant samples were separated into root, stem, leaf, husk, and grain, then dried in a forced-air oven at 80 ºC for at least 72 h. Soil samples were air-dried and sieved with 2 mm mesh.

2.2. Basalt characteristics

Basalt rock was obtained from Kamigassanshita area, Odate city, Akita prefecture, Japan (Horie Kenzai. Ltd., Japan), and crushed in Aichi prefecture (Sobueclay Corporatio, Japan). The basalt

132 characteristics are given in Table 1. The basalt pH was 9.68 and total carbon content was 0.333 g
133 kg^{-1} soil, measured by the protocols below. The particle size distribution was determined using a
134 laser diffraction particle size distribution analyzer (SALD2100, Shimadzu, Kyoto, Japan), and
135 10 %, 50 % and 90 % of particles was smaller than 21.6, 120 and 370 μm, respectively. The
136 mineral content of the basalt used in this study was determined using X-ray powder diffraction
137 (XRPD) analysis using full-pattern summation method (Butler BM and Hillier 2021) following
138 the procedure of Kurokawa et al. (2024). Samples were spiked by 20% with corundum (Al_2O_3) to
139 aid quantitative analysis and ground with ethanol by using XRD-mill (McCrone, Retsch,
140 Germany). The ethanol suspension samples were dried at ambient temperature and reground by
141 using agate pestle and mortar. The XRPD patterns of the powdered samples were obtained by X-
142 ray diffraction (XRD) instrument (MiniFlex600, Rigaku, Tokyo, Japan) using Cu-Kα radiation
143 from 5-65° 2θ, with a step of 0.01° and a scan speed of 10° min^{-1} at 40 kV and 15 mA conditions.
144 The mineral content was calculated from the XRPD patterns using the powdR package (Butler B
145 and Hillier 2020) version 1.3.0 for R language (R Core Team, 2023). The most abundant mineral
146 was bytownite (36.6 wt.%), followed by labradorite (25.7 wt.%) and pyroxene (10.2 wt.%).
147 Bytownite and labradorite are subgroups of plagioclase feldspar, which is a solid solution with a
148 predominance of albite ($NaAlSi_3O_8$) and anorthite ($CaAl_2Si_2O_8$). Bytownite contains 70-90 %
149 anorthite, while labradorite contains 50-70 %. These major minerals in the basalt are easily

150 weathered (Hermanská et al. 2023). The element content of the basalt was determined by energy-
151 dispersive X-ray fluorescence spectroscopy (EDXRF: XEPOSC, SPECTRO Analytical
152 Instruments, Germany) using pressed powder pellet sampling (Table 2). The major elements were
153 SiO_2 (58 wt.%), Al_2O_3 (13 wt.%), Fe_2O_3 (9.9 wt.%), CaO (7.8 wt.%), MgO (4.7 wt.%) and Na_2O
154 (3.8 wt.%). The element contents were considered within the general range when compared to
155 basalts used in a previous study (Lewis et al. 2021).
156

157 **2.3. Potential of element supply from basalt**

158 To evaluate the potential of elemental supply from the basalt used in this study, Si, Ca, Mg, K,
159 and Na were investigated by two extraction methods: (1) shaking for 1 h with 1.0 *M* ammonium
160 acetate solution at a soil solution ratio of 1:20 at ambient temperature followed by filtered with a
161 filter paper (Advantec No. 6) to evaluate elements in exchangeable pool, (2) shaking for 30
162 minutes with 2% citric acid solution at a soil solution ratio of 1:100 at ambient temperature
163 followed by filtered with a filter paper (Advantec No. 6) to evaluate elements potentially dissolved
164 from minerals in rhizosphere (De Medeiros et al. 2021). The elements in the extractions were
165 analyzed by Inductively Coupled Plasma Mass Spectrometry (ICP-MS: ELAN DRC-e,
166 PerkinElmer, Waltham, MA, USA).
167

2.4. Soil chemical analysis

Soils before planting and after harvest were analyzed for pH, soil total carbon, available Si, and exchangeable cations. For soil pH measurements, 3.0 g of soil was weighed into a 50 mL of plastic bottle with 15 mL of Milli-Q water (1:5 mass ratio of soil:water) and shaken for 1 h at ambient temperature (150 rpm; TS-10N, Taitec Co., Ltd, Aichi, Japan). The solution was stood still for 1 h before pH measurement to 0.01 pH units (Kamewada 1997b). Soil total carbon was measured using an elemental analyzer (vario EL cube, Elementar Analysensysteme GmbH, Langenselbold, Germany) following powdered less than 250 μm with pestle and mortar. For available Si measurement, 1.0 g of soil was mixed with 10 mL of 0.02 *M* phosphate buffer solution (sodium dihydrogenphosphate (NaH_2PO_4) : disodium hydrogenphosphate (Na_2HPO_4) = 50:50, pH 6.9) in a 15-mL centrifugation tube and kept in a water bath at 40°C for 5 h. The centrifugation tube was reciprocally shaken 10 times at 40–50 cm width at the beginning of the water bath and again at 0.5, 1, 2, 3, 4 and 5 h after the start of the bath. The solution was then filtered with a filter paper (Advantec No. 6), and the Si concentration of the solution was determined by Inductively Coupled Plasma Atomic Emissions Spectroscopy (ICP-AES: Avio 220 Max, PerkinElmer, Waltham, MA, USA) (Yanai et al. 2016). For soil exchangeable cations, 1.0 g of soil was mixed with 20 mL of 1.0 *M* of ammonium acetate (pH=7.0; 1:20 mass ratio of soil:solution), shaken for 1 h at ambient temperature, filtered with a filter paper (Advantec No. 6) (Kamewada 1997a). The concentrations

of Ca, Mg, K, and Na in the extracts were analyzed using ICP-MS. Total amount of elements in a pot was calculated by multiplying elemental concentration in soil by mass of soil in a pot.

2.5. Rice growth and elemental uptake

Dry weight of each sample was recorded, and samples were analyzed for element concentration according to the method as follows (Ishikawa et al. 2016). Dried samples were powdered using griding mill (Wonder Blender WB-1, Osaka Chemical Co., Ltd., Osaka, Japan). A 70 mg powdered sample was taken to a 65-mL polypropylene tube (DigiTUBE, SCP Sciences, Tokyo, Japan) with 2 mL of a 13 *M* HNO_3 solution (EL grade, Kanto Chemical Inc.) and left for 2 days at ambient temperature, then heated at 105°C for 1.5 h using a heating block system (Digi-PREP, SCP Science, Baie d'Urfé, Quebec, Canada) and cooled to ambient temperature. Then, a 70 mg of the same powdered sample was additionally taken to the same tube, and heated under the same condition and cooled to ambient temperature in order to increase concentration of Si in sample solution to be detected. After that, 0.4 mL of hydrogen peroxide (H_2O_2; atomic-absorption grade, Kanto Chemical Inc.) was added to the solution, which was then heated at 105°C for 0.5 h. The digested solution was adjusted to 10 mL by 2% HNO_3 solution and filtered through a filter paper (Advantec No. 5C). One mL of extracts was diluted to 10 mL by 2% HNO_3 and analyzed for concentrations of Ca, Mg, K, Na, arsenic (As) and heavy metals (cadmium (Cd), copper (Cu),

chromium (Cr), nickel (Ni)) by ICP-MS. To determine Si concentration, the filter papers were washed with hot deionized water, compacted in small melting pots and dried at 80°C for 2 h. Then, they were burned at 550°C in a maffle for 5 h, and the weight of dry ash was measured for Si concentration (Kusa et al. 2021). Elemental uptake in rice was calculated by multiplying elemental concentration in rice by dry weight.

2.6. Calculation of release of Si and cations from the basalt during cultivation

Firstly, change of total amount of elements (Si, Ca, Mg, K, and Na) during cultivation contained by soil and plant in each treatment was calculated. The change of total amount of Si was calculated as follows:

Change of total amount of Si during cultivation (ΔSi) = ($AvailableSi_{AH}$ + $Uptake_{plant}$ of Si) – $AvailableSi_{BP}$ (eq. 3),

where $AvailableSi_{AH}$ is total amount of soil available Si after harvest, $Uptake_{plant}$ of Si is Si uptake in rice, and $AvailableSi_{BP}$ is total amount of soil available Si before planting. Units of change of total amount of Si during cultivation (ΔSi) is represented in g pot^{-1}.

The change of total amount of cations were similarly calculated as follows:

Change of total amount of M during cultivation (ΔM) = (Ex_{AH} of M + $Uptake_{plant}$ of M) – Ex_{BP} of M (eq. 4)

where Ex_{AH} of M is total amount of exchangeable cation in soil after harvest, $Uptake_{plant}$ of M is cation uptake in rice, and Ex_{BP} of M is total amount of exchangeable cation in soil before planting. Units of change of total amount of M during cultivation (ΔM) is represented in g pot^{-1}.

Then, Si and cation release from the basalt in each treatment was calculated by subtracting the change of total amount of each element during cultivation in B0 from that in each treatment to eliminate the input from tap water and natural weathering of the mineral originally existed in the soil (Ten Berge et al. 2012). As an example of Si release from the basalt in B100, the calculation was as follows:

$$\text{Release of Si from the basalt} = (\Delta Si_{100} - \Delta Si_0) / (\text{M.W. of Si} \times 1000), \quad \text{(eq. 5)}$$

where ΔSi_{100} is the change of total amount of Si during cultivation in B100 (g pot^{-1}), ΔSi_0 is the change of total amount of Si during cultivation in B0 (g pot^{-1}), and M.W. of Si is molar weight of Si (28.1 g mol^{-1}). Units of release of Si is represented in mmol pot^{-1}. As for ΔSi_0, the mean value was used in the calculation. Release of cations from the basalt was also calculated based on (eq.5).

2.7. Calculation of carbon balance in the soil and in the whole system

Carbon balance in the soil and in the whole system was calculated as follows:

$$\text{Carbon balance in the soil} = TC_{AH} - TC_{BP} \quad \text{(eq. 6)}$$

$$\text{Carbon balance in the whole system} = (TC_{AH} - TC_{BP}) + [TC_{plant}] \times DW_{plant} \quad \text{(eq. 7)}$$

where TC_{AH} is total amount of total carbon in the soil after harvest (gC pot^{-1}), TC_{BP} is total amount of total carbon in the soil before planting (gC pot^{-1}), [TC_{plant}] is total carbon concentration in plant (0.413 g g^{-1} plant, Naser et al. 2020), and DW_{plant} is total dry weight of rice (g $plant^{-1}$). Units of carbon balance is represented in gC pot^{-1}.

2.8. Statistical analysis

Statistical differences between the element concentration of extracts from the basalt and soil were examined by Welch's t-test. Significant differences in soil pH, total amount of elements in soil, dry weight of plant, elemental uptake in plant, element concentration in grain, cation release from the basalt, carbon balance in the soil and in the whole system were determined and compared among application rates of the basalt using one-way ANOVA and Tukey post hoc tests. The Pearson product moment correlation coefficient (R) was used to examine the correlation of the total amount of available Si in the soil with the uptake of Si in rice and dry weight, as well as the total amount of exchangeable Na in the soil with the uptake of Na in rice and dry weight. Outliers were statistically determined by the Smirnov–Grubbs test and excluded from the experimental analysis. All statistical analysis were performed using the computing environment R (R Core Team, 2023).

3. Results

3.1. Potential of elemental supply from basalt

Element concentrations of the basalt by two extraction methods are shown in Table 3, as well as the soil of B0 before planting. Si and Na were higher in the basalt than in the soil in both extraction methods, whereas K was lower in the basalt than in the soil. Ca was higher in the basalt in 1.0 *M* ammonium acetate extraction than in the soil, but showed no difference in 2 % citric acid extraction. Mg was lower in the basalt in 1.0 *M* ammonium acetate extraction, but higher in 2 % citric acid extraction than in the soil.

3.2. Soil chemical properties with different application rates of basalt

The soil chemical properties before planting and after harvest are shown in Table 4 and Supplemental table 1. Soil pH before planting increased with the higher basalt application rate and was significantly higher in B50 and B100 than other treatments. Total amount of soil total carbon, exchangeable Mg and K before planting showed no difference among the treatments. Total amount of soil available Si and exchangeable Ca in pot before planting showed significant difference by one-way ANOVA, and lowest in B5 and highest in B100. Total amount of soil exchangeable Na in pot before planting significantly increased with the higher basalt application

rate. On the other hand, soil pH and total amount of soil total carbon after harvest didn't differ among the treatment. Total amount of soil available Si, exchangeable Mg and Na in pot after harvest significantly increased with the higher basalt application rate. Total amount of soil exchangeable Ca and K in pot after harvest showed no significant difference among the treatments. Basically, the exchangeable K and Mg concentration and Mg:K ratio in soil before planting and after harvest were higher than the diagnostic standard for paddy field fertilization in Hokkaido prefecture, i.e. 124 mg kg^{-1} soil for exchangeable K, 151 mg kg^{-1} soil for exchangeable Mg, and 2 in equivalent ratio for Mg:K ratio (Hokkaido Research Organization 2020) (supplemental table 1). The available Si concentration extracted by phosphate buffer solution was higher than 34.4 mg kg^{-1} soil, which is the average in Gray Lowland soil in Japan (Yanai et al. 2016).

3.3. Rice growth and element uptake responding to basalt application

The dry weight of each part of rice is shown in Table 5. No significant difference was observed in dry weight of each part nor total of them among the treatments. There were no significant differences in yield-related indexes among the treatments either (Supplemental table 2). Table 6 shows the total uptake of Si, Ca, Mg, K and Na in rice. The uptake of Si showed significant difference among the treatments by one-way ANOVA ($p < 0.05$), and Si uptake increased with the higher basalt application rate. The uptake of Ca, Mg, and K didn't show significant difference

among the treatments, but the uptake of Na significantly increased with the higher basalt application rate ($p < 0.01$). Table 7 shows the concentration of As, Cd, Cu, Cu, and Ni in grain, and no significant difference was detected among the application rates of the basalt.

3.4. Si and cation release from basalt during cultivation

Release of Si, Ca, Mg, K, and Na from the basalt are shown in Figure 1. Si release differed among the application rates and significantly increased with the higher application rates of the basalt. Ca release from the basalt didn't differ among the application rate of basalts. Mg release significantly increased with the higher application rates of the basalt. K release showed significant difference among the application rates by one-way ANOVA and was lower in B20. Na release showed significant difference among the application rates by one-way ANOVA and increased with the higher application rates of basalt.

3.5. Carbon balance in the soil and in the whole system

Carbon balance in the soil, total amount of carbon in plant, and carbon balance in the whole system are shown in Table 8. Carbon balance in the soil showed significant difference among the treatments by one-way ANOVA. Total amount of carbon in plant nor carbon balance in the

whole system didn’t differ among the treatments.

4. Discussion

4.1. Impact of basalt application on soil chemical properties and elemental uptake in rice

The application of the basalt increased total amount of soil available Si before planting, after harvest and the uptake of Si in rice (Table 4 and 6), and positive correlation was detected between them (Figure 2(a)). The available Si in this study was extracted by the phosphate buffer solution, and is considered monosilicate adsorbed on the surface of soil particles and easily desorbed and supplied to plants (Shigezumi et al. 2002). Therefore, the results in this experiment suggested that silicate minerals in the basalt got weathered during cultivation and supplied monosilicate to the surface of soil particles and soil solutions as available Si, which was partly absorbed by rice plant. Wang et al (2024) also reported the increase of available Si concentration in soil and Si concentration in paddy rice straw by application of wollastonite as well as this study, which confirms easily weatherable silicate mineral application is effective to supply Si to soil and plant in paddy rice field. Moreover, total amount of soil available Si after harvest was also positively correlated with total dry weight of rice, even though dry weight itself didn't significantly differ among the treatments (Table 5 and Figure 2(b)). Since Si has physical and chemical stress-relieving effects in rice, such as reducing salt and heat stress, improving physical strength and light-receiving attitude (Ma 2004; Ma. and Yamaji 2008), the increase of available Si in soil and its uptake by rice could have contributed to rice growth in this study. Further, as the beneficial

effects of Si have been observed not only in rice but also other crops regardless of monocotyledonous or dicotyledonous plants (Fawe et al. 1998; Tripathi et al. 2021), Si supply can be one of the important co-benefits in ERW strategy.

The application of basalt increased total amount of soil exchangeable Ca before planting and after harvest by just 5 to 7 % even in B100, the highest application treatment, compared with B0 (Table 4), which was unexpectable because the basalt contained easily weatherable Ca-rich minerals including bytownite and labradorite. This was probably attributed to the relatively high exchangeable Ca content in the soil used in this study (Table 3). On the other hand, the application of basalt increased total amount of soil exchangeable Mg after harvest (Table 4). Since total amount of soil exchangeable Mg didn't differ among the basalt application rate before planting, the increase of Mg probably derived from the weathering of the basalt during cultivation. Since soil exchangeable Mg concentration didn't increase by wollastonite application in paddy field (Wang et al., 2024), Mg supply was revealed to be a beneficial effect of basalt application compared to wollastonite application. The increase of soil exchangeable Mg didn't affect the uptake of Mg in rice (Table 6), probably because the soil used in this study contained higher exchangeable Mg than the diagnostic standard for fertilization (Hokkaido Research Organization 2020) and was fertile enough to meet Mg demand by rice even without the basalt application. If basalt is applied to a field with low exchangeable Mg concentration, Mg uptake by plant can be

348 enhanced by basalt application, possibly leading to growth promotion.

349 Moreover, the application of the basalt increased the total amount of soil exchangeable Na
350 before planting, after harvest, and the uptake of Na in rice (Table 4 and 6). There was a positive
351 correlation between the total amount of soil exchangeable Na after harvest and the uptake of Na
352 in rice (Figure 3(a)), suggesting the increase of total amount of soil exchangeable Na caused the
353 increase of Na uptake in rice plants. However, rice is susceptible to Na salinity, and high Na
354 concentration in soil antagonistically inhibits K uptake by rice and interferes metabolism because
355 of ion imbalance in a cell (Coca et al. 2023). The threshold of EC of soil water is 3 dS/m (≈ 30
356 m*M* of NaCl) for rice (Chinnusamy et al. 2005), and salt stress reduces yield mainly due to the
357 reduction in the number of tillers and spikelets per panicle (Zeng and Shannon 2000). Fortunately,
358 there was no correlation between total dry weight of rice and the total amount of soil exchangeable
359 Na (Figure 3(b)) and no significant decrease by basalt application was observed in yield-related
360 indices (supplemental table 2), suggesting Na concentration in soil wasn't high enough to inhibit
361 rice growth in this study. Also, as Na is monovalent cation and relatively easy to be leached
362 (Gillman et al. 2001), it is less possible that Na supply from the basalt negatively affects rice
363 growth in paddy field, where water derived from river leaches downward during most of the
364 cultivation season. However, as basalt generally contains Na in easily weatherable plagioclase
365 minerals, the effect of basalt application in paddy field should be carefully monitored particularly

366 in the case of continuous application, with high application rate, or application to the area where
367 soil Na salinity is originally high.

368 The increase of concentrations of As, Cd, Cu, Cr, and Ni in rice grain by the basalt application
369 was not observed (Table 7), which reflected that the basalt contained low amount of heavy metals
370 (Beerling et al. 2018). Kelland et al. (2020) also reported no significant increase in As and heavy
371 metal elements concentration in sorghum grain by application of the basalt in upland condition
372 and the consistent result was obtained even under submerged paddy condition. On the other hand,
373 Vienne et al. (2022) reported the increase of exchangeable Ni concentration in soil and Ni
374 concentration in soil solution by basalt application in potato cultivation. Since the mobility of
375 these elements are affected by soil pH, redox conditions, and organic matter contents (El-Naggar
376 et al. 2021; Kumar et al. 2021; Zulfiqar et al. 2023), it is necessary to consider the difference of
377 soil properties, management practice, and the basalt characteristics to be applied, and to be careful
378 in assessing the risk of pollution by As and heavy metal elements in ERW strategy.

379 As for soil pH, the basalt application increased soil pH before planting, but didn't affect soil
380 pH after harvest (Table 4). In paddy field, it is known that soil solution pH converges to around
381 7.0 because production and consumption of protons come to be balanced over time by the
382 dissolution of carbon dioxide and the reduction of trivalent iron to divalent iron in soil,
383 respectively (Sahrawat 2005), and the soil pH after harvest were probably affected by the soil

384 solution pH convergence.

385

386 **4.2. Basalt weathering and release of Si and cations during cultivation**

387 The increase of the release of Si, Mg and Na from the basalt during cultivation corresponded to
388 the increase of the basalt application rate, which indicated the weathering of the basalt occurred
389 during cultivation (Figure 1(a),(c),(e)). These results were consistent with the mineralogical
390 characteristic of the basalt, containing 10.2 wt.% of pyroxene and 62.3 wt.% of plagioclase
391 (bytownite and labradorite) (Table 1). Pyroxene contains Si and Mg while plagioclase contains Si
392 and Na, and both are easy to be weathered especially in the presence of plant (Moulton et al.
393 2000). The result of 2 % citric acid extraction also showed higher Si, Mg and Na concentration in
394 the basalt than the soil, supporting the result of the release of these elements from the basalt by
395 weathering (Table 3). On the other hand, the release of Ca didn't show the significant difference
396 among the application rates (Figure 1(a)) though Ca-containing silicate minerals like plagioclase
397 and pyroxene were presumed to be weathered. Considering the high exchangeable Ca content in
398 the soil used in this study (Table 3), it might be possible that Ca in soil water reached saturation
399 during cultivation and precipitated as secondary mineral and calcium salt which was insoluble in
400 1.0 *M* ammonium acetate. The release of K showed significant differences among the treatments
401 by one-way ANOVA but the reason for the negative value of K release in B20 treatment was

unclear (Figure 1(c)). In any case, since the basalt used in this study contained little K (Table2), K was probably hardly supplied from the basalt.

When we compared the rate for Mg and Na release with the previous study by Kelland et al. (2020), in which sorghum was cultivated in a pot under upland condition, the rate for Mg release in B100 (6.5 mmol m^{-2} day^{-1}) was similar order of magnitude to that observed in Kelland et al. (2020) (4.2 mmol m^{-2} day^{-1} in 100 t ha^{-1} application of basalt) (Supplemental table 3). This result suggests that paddy rice cultivation with basalt powder has the comparable ERW potential with their study. Based on (eq. 1 and 2), gross sequestration by the basalt weathering amounts to 0.012 g C per mmol of Mg in the form of carbonate precipitation, and if 100 t ha^{-1} of the basalt powder is applied to all of paddy field in Japan (2,319,000 ha) (Ministry of Agriculture, Forestry and Fisheries. 2024) and weathered in a rate of 6.5 mmol m^{-2} day^{-1}, the sequestrated carbon by the basalt weathering will be 663,234 t CO_2 in one cultivation cycle (99 days) in Japan. Moreover, rate for Na release in B100 (4.6 mmol m^{-2} day^{-1}) was one order of magnitude higher than that observed in Kelland et al. (2020) (0.33 mmol m^{-2} day^{-1}) (Supplemental table 3), indicating the weathering of the basalt used in this study can release considerable amount of Na, not only Mg. Since Na cannot precipitate as carbonate in water because of its high solubility, it cannot sequestrate carbon directly. However, Na electrically binds to nitric and sulfuric acid which derive from fertilizer and may help increase the alkalinity of leachate from agricultural land and maintain

420 the alkalinity of rivers and oceans (Renforth and Henderson 2017; Kelland et al. 2020).

421

422 **4.3. Carbon balance in the soil and in the whole system**

423 Carbon balance in the soil significantly differed among the treatments by one-way ANOVA
424 (Table 8). However, the difference of the carbon balance didn't correspond to the application rate
425 of the basalt. This result suggests that the basalt weathering didn't affect carbon balance in the
426 soil, though we observed the release of Mg and Na from the basalt. Based on (eq. 1), 32 mmol of
427 Mg release from the basalt in B100 treatment only equaled to 0.77 g C pot^{-1} even if all of Mg
428 released from the basalt contributed to carbon sequestration. Therefore, the potential of additional
429 inorganic carbon storage was less than 0.5 % of total amount of soil total carbon in pot at most,
430 which was little to detect its impact on carbon balance. Moreover, the mean value of total amount
431 of carbon in plant increased by the basalt application, but didn't significantly differ among the
432 treatments, neither did carbon balance in the whole system, which was calculated as the sum of
433 the carbon balance in the soil and total amount of carbon in plant (Table 8).

434 In this study, we couldn't detect the carbon sequestration by the basalt application probably
435 because of the insufficient amount of weathering of the basalt in 99 days of cultivation. However,
436 rock weathering continues to occur over time and its impact should be evaluated in longer-term.
437 In addition, most of previous studies of ERW have been conducted assuming aerobic field

condition. However, quite different biogeochemical reactions happen in paddy field under anaerobic environment. For example, ferric (Fe^{3+}) ions in mineral structure can be reduced to ferrous (Fe^{2+}) ions due to anaerobic condition and result in enhancement of weathering as ferrous ion is much more soluble than ferric ion, whereas an increase in HCO_3^- in the soil solution due to mineral weathering could lead to the release of methane (CH_4) gas by increasing the reaction substrate for methanogenic bacteria. As a future perspective, it is necessary to evaluate the potential of basalt application on carbon sequestration considering the unique carbon dynamics to paddy field condition in long term.

5. Conclusion

We observed the application of the basalt supplied elements to the soil and paddy rice. The application of the basalt increased soil available Si, exchangeable Mg and Na in this study. Moreover, the soil available Si had positive correlation with Si uptake in rice and dry weight of rice, suggesting an increase of soil available Si by the basalt application can contribute to rice growth due to an increase of Si uptake and its stress-relieving effect. Also, the release of Si, Mg, and Na from the basalt showed the weathering of the applied basalt during 99 days of paddy rice cultivation. The potential of basalt application on the supply of several available nutrients was firstly demonstrated in submerged paddy condition and longer-term experiment will be necessary to prove its potential for carbon sequestration.

Acknowledgements

This research was executed with the financial support of the New Energy and Industrial Technology Development Organization (NEDO), project no. JPNP18016 “Advanced enhanced rock weathering (A-ERW) technology actively combined with site characteristics”. Additional support was provided by the Japan Science and Technology Agency (JST), project no. JPMJSP2119 “Support for Pioneering Research Initiated by the Next Generation (SPRING)”.

We thank Takumi Inoue for assisting experiment preparation and sampling. We acknowledge Horie Kenzai. Ltd. and Sobueclay corporation for kindly preparing and providing basalt powder.

Disclosure statement

No potential conflict of interest was reported by the authors.

Funding

This work was supported by the New Energy and Industrial Technology Development Organization under Grant JPNP18016; and the Japan Science and Technology Agency under Grant JPMJSP2119.

475

References

Amann T, Hartmann J, Struyf E, De Oliveira Garcia W, Fischer EK, Janssens I, Meire P, Schoelynck J. 2020. Enhanced Weathering and related element fluxes – a cropland mesocosm approach. Biogeosciences. 17(1):103-119. doi:10.5194/bg-17-103-2020

Anda M, Shamshuddin J, Fauziah C. 2015. Improving chemical properties of a highly weathered soil using finely ground basalt rocks. Catena. 124:147-161. doi:10.1016/j.catena.2014.09.012

Andrews MG, Taylor LL. 2019. Combating Climate Change Through Enhanced Weathering of Agricultural Soils. Elements. 15(4):253-258. doi:10.2138/gselements.15.4.253

Beerling DJ, Kantzas EP, Lomas MR, Wade P, Eufrasio RM, Renforth P, Sarkar B, Andrews MG, James RH, Pearce CR et al. 2020. Potential for large-scale CO2 removal via enhanced rock weathering with croplands. Nature. 583(7815):242-248. doi:10.1038/s41586-020-2448-9

Beerling DJ, Leake JR, Long SP, Scholes JD, Ton J, Nelson PN, Bird M, Kantzas E, Taylor LL, Sarkar B et al. 2018. Farming with crops and rocks to address global climate, food and soil security. Nature Plants. 4(3):138-147. doi:10.1038/s41477-018-0108-y

Butler B, Hillier S. 2020. powdR: full pattern summation of X-ray powder diffraction data. R package version. 1(1). doi:10.32614/CRAN.package.powdR

494 Butler BM, Hillier S. 2021. powdR: An R package for quantitative mineralogy using full pattern
495 summation of X-ray powder diffraction data. Computers & Geosciences. 147.
496 doi:10.1016%2Fj.cageo.2020.104662
497 Chinnusamy V, Jagendorf A, Zhu JK. 2005. Understanding and Improving Salt Tolerance in
498 Plants. Crop Science. 45(2):437-448. doi:10.2135/cropsci2005.0437
499 Coca L, González M, Unday Z, Hernández J, Jáuregui M, Cancio Y. 2023. Effects of Sodium
500 Salinity on Rice (*Oryza sativa* L.) Cultivation: A Review. SUSTAINABILITY.
501 doi:10.3390/su15031804
502 Conrad R. 2007. Microbial ecology of methanogens and methanotrophs. ADVANCES IN
503 AGRONOMY, VOL 96. p. 1-63. doi:10.1016/S0065-2113(07)96005-8
504 De Medeiros DS, Sanchotene DM, Ramos CG, Oliveira LFS, Sampaio CH, Kautzmann RM.
505 2021. Soybean crops cultivated with dacite rock by-product: A proof of a cleaner
506 technology to soil remineralization. Journal of Environmental Chemical Engineering.
507 9(6):106742. doi:10.1016/j.jece.2021.106742
508 El-Naggar A, Ahmed N, Mosa A, Niazi NK, Yousaf B, Sharma A, Sarkar B, Cai YJ, Chang SX.
509 2021. Nickel in soil and water: Sources, biogeochemistry, and remediation using biochar.
510 Journal of Hazardous Materials. 419. doi:10.1016/j.jhazmat.2021.126421
511 Fawe A, Abou-Zaid M, Menzies JG, Bélanger RR. 1998. Silicon-mediated accumulation of

512 flavonoid phytoalexins in cucumber. Phytopathology. 88(5):396-401.
513 doi:10.1094/phyto.1998.88.5.396
514 Food and Agriculture Organization of the United Nations (FAO). 2022. Top production
515 quantity—World (total) in 2022. FAOSTAT statistical database.
516 https://www.fao.org/faostat/en/#data
517 Gillman GP, Burkett DC, Coventry RJ. 2001. A laboratory study of application of basalt dust to
518 highly weathered soils: effect on soil cation chemistry. Soil Research. 39(4):799.
519 doi:10.1071/sr00073
520 Hansen J, Sato M, Kharecha P, Von Schuckmann K, Beerling DJ, Cao J, Marcott S, Masson-
521 Delmotte V, Prather MJ, Rohling EJ et al. 2017. Young people's burden: requirement of
522 negative CO_2 emissions. Earth System Dynamics. 8(3):577-616. doi:10.1071/sr00073
523 Haque F, Santos RM, Chiang YW. 2020. Optimizing Inorganic Carbon Sequestration and Crop
524 Yield With Wollastonite Soil Amendment in a Microplot Study. Frontiers in Plant Science.
525 11. doi:10.3389/fpls.2020.01012
526 Haque F, Santos RM, Dutta A, Thimmanagari M, Chiang YW. 2019. Co-Benefits of
527 Wollastonite Weathering in Agriculture: CO_2 Sequestration and Promoted Plant Growth.
528 ACS Omega. 4(1):1425-1433. doi:10.1021/acsomega.8b02477
529 Hermanská M, MJ Voigt, C Marieni, J Declercq, and EH Oelkers. 2023. A comprehensive and

consistent mineral dissolution rate database: Part II: Secondary silicate minerals. CHEMICAL GEOLOGY 636. doi: 10.1016/j.chemgeo.2023.121632.

Hokkaido Research Organization. 2020. Hokkaido Fertilizer Recommendations 2020. 1-226. Hokkaido Government Department of Agriculture.

Intergovernmental Panel on Climate Change (IPCC). 2023. AR6 Synthesis Report Climate change 2023. https://www.ipcc.ch/report/ar6/syr/

Ishikawa S, Makino T, Ito M, Harada K, Nakada H, Nishida I, Nishimura M, Tokunaga T, Shirao K, Yoshizawa C et al. 2016. Low-cadmium rice (*Oryza sativa* L.) cultivar can simultaneously reduce arsenic and cadmium concentrations in rice grains. Soil Science and Plant Nutrition. 62(4):327-339. doi:10.1080/00380768.2016.1144452

IUSS Working Group WRB. 2022. World reference base for soil resources. International soil classification system for naming soil sand creating legends for soil maps (4th ed.). International Union of Soil Sciences (IUSS). https://wrb.isric.org/

Kamewada K. 1997a. Chapter V.7, Exchangeable cations and anions. In: *Dojo-Kankyo-Bunseki-Ho (analytical Methods for Soil Environment)*. Tokyo: Hakuyusya; p. 215-222.

Kamewada K. 1997b. Chapter V.1, pH (glass electrode method). In: *Dojo-Kankyo-Bunseki-Ho (analytical Methods for Soil Environment)*. Tokyo: Hakuyusya; p. 195-197.

Kaneta Y. 2019. Recent changes in paddy soils and strategy for sustainable rice production.

548 Jounal of the Japanese Society of Soil Physics. 141(0):41-48.
549 doi:10.34467/jssoilphysics.141.0_41
550 Kantola IB, Blanc-Betes E, Masters MD, Chang E, Marklein A, Moore CE, Von Haden A,
551 Bernacchi CJ, Wolf A, Epihov DZ et al. 2023. Improved net carbon budgets in the US
552 Midwest through direct measured impacts of enhanced weathering. Global Change
553 Biology. 29(24):7012-7028. doi:10.1111/gcb.16903
554 Kantola IB, Masters MD, Beerling DJ, Long SP, Delucia EH. 2017. Potential of global
555 croplands and bioenergy crops for climate change mitigation through deployment for
556 enhanced weathering. Biology Letters. 13(4):20160714. doi: 10.1098/rsbl.2016.0714
557 Kelland ME, Wade PW, Lewis AL, Taylor LL, Sarkar B, Andrews MG, Lomas MR, Cotton
558 TEA, Kemp SJ, James RH et al. 2020. Increased yield and CO_2 sequestration potential with
559 the C_4 cereal *Sorghum bicolor* cultivated in basaltic rock dust-amended agricultural soil.
560 Global Change Biology. 26(6):3658-3676. doi:10.1111/gcb.15089
561 Kumar A, Jigyasu DK, Subrahmanyam G, Mondal R, Shabnam AA, Cabral-Pinto MMS,
562 Malyan SK, Chaturvedi AK, Gupta DK, Fagodiya RK et al. 2021. Nickel in terrestrial
563 biota: Comprehensive review on contamination, toxicity, tolerance and its remediation
564 approaches. Chemosphere. 275. doi:10.1016/j.chemosphere.2021.129996
565 Kurokawa K, Azuma K, Nakao A, Suzuki A, Wakabayashi S, Fujimura S, Shinano T, Yanai J.

2024. Examination of the reliability of X-ray powder diffraction analysis to determine mineral composition of soils. Soil Science Society of America Journal. 88(6): 1942-1958. doi:10.1002/saj2.20757

Kusa K, Moriizumi M, Hobara S, Kaneko M, Matsumoto S, Kasuga J, Ae N. 2021. Mineral weathering and silicon uptake by rice plants promote carbon storage in paddy fields. Soil Science and Plant Nutrition. 67(2):162-170. doi:10.1080/00380768.2021.1878471

Ma JF, Yamaji N. 2008. Functions and transport of silicon in plants. Cellular and Molecular Life Sciences. 65(19):3049-3057. doi:10.1007/s00018-008-7580-x

Ma JF. 2004. Role of silicon in enhancing the resistance of plants to biotic and abiotic stresses. Soil Science and Plant Nutrition. 50(1):11-18. doi:10.1080/00380768.2004.10408447

Meharg A, Williams P, Adomako E, Lawgali Y, Deacon C, Villada A, Cambell R, Sun G, Zhu Y, Feldmann J et al. 2009. Geographical Variation in Total and Inorganic Arsenic Content of Polished (White) Rice. Environmental Science & Technology. 43(5):1612-1617. doi:10.1021/es802612a

Ministry of Agriculture, Forestry and Fisheries. 2024. Statistics of agricultural land area.

Moulton K, West A, Berner R. 2000. Solute flux and mineral mass balance approaches to the quantification of plant effects on silicate weathering. AMERICAN JOURNAL OF SCIENCE. p. 539-570. doi:10.2475/ajs.300.7.539

584 Nakamura T, Osaki M, Watanabe T. 2024. Zero-valent iron reduces cadmium and arsenic
585 accumulation in spinach (*Spinacia oleracea* L.). JOURNAL OF PLANT NUTRITION. p.
586 646-655. doi:10.1080/01904167.2023.2280151
587 Naser HM, Nagata O, Sultana S, Hatano R. 2020. Carbon Sequestration and Contribution of
588 CO_2, CH_4 and N_2O Fluxes to Global Warming Potential from Paddy-Fallow Fields on
589 Mineral Soil Beneath Peat in Central Hokkaido, Japan. Agriculture-Basel. 10(1).
590 doi:10.3390/agriculture10010006
591 Obara H, Ohkura T, Takata Y, Kohyama K, Maejima Y, and Hamazaki T. 2011. Comprehensive
592 Soil Classification System of Japan First Approximation. BULLETIN OF NATIONAL
593 INSTITUTE FOR AGRO-ENVIRONMENTAL SCIENCES. 29:1-73.
594 Renforth P, Henderson G. 2017. Assessing ocean alkalinity for carbon sequestration. Reviews of
595 Geophysics. 55(3):636-674. doi:10.1002/2016rg000533
596 Sahrawat K. 2005. Fertility and organic matter in submerged rice soils. CURRENT SCIENCE.
597 p. 735-739. doi: 10.1300/J064v31n03_03
598 Shigezumi M, Kitta Y, Kubo S, Mizuochi T. 2002. The evaluation of the available silica in
599 paddy soil by the phosphate buffer extraction method. Japanese Journal of Soil Science and
600 Plant Nutrition. 73(4):383-390. doi:10.20710/dojo.73.4_383
601 Swoboda P, Döring TF, Hamer M. 2022. Remineralizing soils? The agricultural usage of silicate

rock powders: A review. Science of the Total Environment. 807.
doi:10.1016/j.scitotenv.2021.150976

Ten Berge HFM, Van Der Meer HG, Steenhuizen JW, Goedhart PW, Knops P, Verhagen J. 2012. Olivine Weathering in Soil, and Its Effects on Growth and Nutrient Uptake in Ryegrass (*Lolium perenne* L.): A Pot Experiment. PLoS ONE. 7(8):e42098.
doi:10.1371/journal.pone.0042098

Tripathi P, Na CI, Kim Y. 2021. Effect of silicon fertilizer treatment on nodule formation and yield in soybean (*Glycine max* L.). European Journal of Agronomy. 122.
doi:10.1016/j.eja.2020.126172

Vienne A, Poblador S, Portillo-Estrada M, Hartmann J, Ijiehon S, Wade P, Vicca S. 2022. Enhanced Weathering Using Basalt Rock Powder: Carbon Sequestration, Co-benefits and Risks in a Mesocosm Study With Solanum tuberosum. Frontiers in Climate. 4.
doi:10.3389/fclim.2022.869456

Wang FN, Zhu FF, Liu DZ, Qu YY, Liu D, Xie J, Wang A, Kang RH, Quan Z, Li YH et al. 2024. Wollastonite powder application increases rice yield and CO_2 sequestration in a paddy field in Northeast China. Plant and Soil. doi:10.1007/s11104-024-06570-5

Yanai J, Taniguchi H, Nakao A. 2016. Evaluation of available silicon content and its determining factors of agricultural soils in Japan. Soil Science and Plant Nutrition. 62(5-

6):511-518. doi:10.1080/00380768.2016.1232601

Yang Y, Kosaka G, Uchibayashi H, Zhu Y, Kuromochi K, Shinano T, Watanabe T, Maruyama H, Hamamoto S, Nakao A, Toma Y. 2024. Enhanced CO2 removal and improved carbon budget by enehaned rock weathering: A field experiment in Hokkaido, Japan. Nutrient Cycling in Agroecosystem. (submitted)

Zeng L, Shannon MC. 2000. Salinity Effects on Seedling Growth and Yield Components of Rice. Crop Science. 40(4):996-1003. doi:10.2135/cropsci2000.404996x

Zulfiqar U, Haider FU, Ahmad M, Hussain S, Maqsood MF, Ishfaq M, Shahzad B, Waqas MM, Ali B, Tayyab MN et al. 2023. Chromium toxicity, speciation, and remediation strategies in soil-plant interface: A critical review. Frontiers in Plant Science. 13. doi:10.3389/fpls.2022.1081624

Figure legends

Figure 1. Release of Si (a), Ca (b), Mg (c), K (d), and Na (e) from basalt during cultivation. Points represent mean values ± one standard error (n=4). “ANOVA” shows the results of one-way ANOVA, which was performed to detect the significant differences among the application rates of basalt. Asterisks (*,**,***) denotes $p < 0.05$, 0.01, 0.001, respectively. “n.s.” denotes not significant ($p > 0.05$). Different letters indicate significant differences among the application

638 rates of basalt determined via Tukey post hoc test.

639 **Figure 2.** Relationship between total amount of soil available Si after harvest and Si uptake in

640 rice **(a)** and total dry weight **(b)**. **(a)** Points represent values of each sample. Linear regression

641 analysis was performed. *R* denotes the Pearson product moment correlation coefficient.

642 Asterisks (***) denotes $p < 0.001$. **(b)** Points represent values of each sample. Linear regression

643 analysis was performed. *R* denotes the Pearson product moment correlation coefficient.

644 Asterisks (**) denotes $p < 0.01$.

645 **Figure 3.** Relationship between total amount of soil exchangeable Na after harvest and Na

646 uptake in rice **(a)** and total dry weight **(b)**. **(a)**Points represent values of each sample. Linear

647 regression analysis was performed. *R* denotes the Pearson product moment correlation

648 coefficient. Asterisks (***) denotes $p < 0.001$. **(b)**Points represent values of each sample. Linear

649 regression analysis was performed. *R* denotes the Pearson product moment correlation

650 coefficient. No significance was observed ($p > 0.05$).

651

652 **Table legends**

653 **Table 1.** Characteristics of basalt

654 **Table 2.** Total elemental composition of basalt used in experiment, derived from XRF runs

655 **Table 3.** Element concentrations of basalt and soil by two extraction methods

656 **Table 4.** Soil chemical properties before planting and after harvest

657 **Table 5.** Dry weight of each part of rice at harvest

658 **Table 6.** Total uptake of elements in rice

659 **Table 7.** Concentrations of As and heavy metals in grain of rice

660 **Table 8.** Carbon balance between before planting and after harvest in the soil and in the whole

661 system

662

663 **Supplemental information legends**

664 **Supplemental figure 1.** Schematic diagram of the pot **(a)** and photograph of status of the

665 experiment on 20th August 2022 (2 months in) **(b)** and on 22nd September (at harvest) **(c)**.

666 **Supplemental table 1.** Element concentration in soil. Mean values ± one standard error are

667 shown. Sample size before planting was three, while after harvest was four. “ANOVA” the

668 results of one-way ANOVA, which was performed for detecting the significant differences

669 among the application rate of basalt. Asterisks (*,**,***) denote $p < 0.05$, 0.01, 0.001,

670 respectively. “n.s.” denotes not significant ($p > 0.05$). Different letters indicate significant

differences among the treatments determined via Tukey post hoc test.

Supplemental table 2. Yield-related indexes of rice. Mean values ± one standard error are shown (n=4). “ANOVA” shows the results of one-way ANOVA, which was performed for detecting the significant differences among the application rate of basalt. “n.s.” denotes not significant ($p > 0.05$). No significant difference among the treatments was determined via Tukey post hoc test.

Supplemental table 3. Release rate of Ca, Mg, Na and K from the basalt. Mean values ± one standard error are shown (n=4). “wt. %” means the proportion of applied basalt powder to soil mixed with by weight. The surface area of the pot was 0.05 m^{-2} and the cultivation duration was 99 days.

684 **Table 1.** Characteristics of basalt

Chemical properties	
pH(H_2O)	9.68
TC (g kg^{-1} soil)	0.333
Particle size distribution (μm)	
D10	21.6
D50	120
D90	370
Mineralogical composition (wt.%)	
Bytownite	36.6
Labradorite	25.7
Pyroxene	10.2
Magnetite	6.77
Smectite	5.64
Cristobalite	4.45
Quartz	4.10
Olivine	4.27
Oligoclase	2.25

685 "TC" means total carbon. D10, 50, 90 means 10 %, 50 %, 90 % of particles was smaller than
686 the given diameter, respectively.

687

688 **Table 2.** Total elemental composition of basalt used in experiment, derived from energy-
689 dispersive X-ray fluorescence spectroscopy runs

Oxide	Content (wt.%)	Element	Content (mg kg^{-1})
SiO_2	58 ± 0	As	0.21 ± 0.00
Al_2O_3	13 ± 0	Ba	166 ± 8
Fe_2O_3	9.9 ± 0.0	Cd	0.43 ± 0.40
CaO	7.8 ± 0.0	Cl	75 ± 3
MgO	4.7 ± 0.0	Co	1.0 ± 0.0
Na_2O	3.8 ± 0.1	Cr	29 ± 0
K_2O	0.34 ± 0.00	Cu	28 ± 1
P_2O_5	0.22 ± 0.00	Hg	0.94 ± 1.27
TiO_2	0.81 ± 0.00	Mo	0.21 ± 0.00
MnO	0.15 ± 0.00	Ni	8.3 ± 0.9
SO_3	0.00 ± 0.00	Pb	10 ± 0
		Rb	13 ± 0
		Sn	1.8 ± 0.3
		Sr	206 ± 2
		V	249 ± 2
		Zn	66 ± 1

690 Mean values ± one standard division are shown (n=3).

691

692 **Table 3.** Element concentrations of basalt and soil by two extraction methods

Element	1.0 *M* ammonium acetate (mg kg^{-1})			2 % citric acid (mg kg^{-1})		
	basalt	soil		basalt	soil	
Si	82.3 ± 10.4	30.0 ± 5.2	*	565 ± 25	169 ± 11	**
Ca	5033 ± 26	4600 ± 44	**	4185 ± 50	4014 ± 264	
Mg	385 ± 2	512 ± 6	**	946 ± 16	545 ± 30	**
K	90.2 ± 1.6	592 ± 27	***	87.6 ± 0.7	506 ± 4	***
Na	1575 ± 13	45.5 ± 7.9	***	1611 ± 16	50.6 ± 5.7	***

693 Mean values ± one standard error are shown (n=3). Welch's t-test was performed to detect the significant differences of element concentrations in
694 each extract between the basalt and the soil of B0 before planting. Asterisks (*, **, ***) denote $p < 0.05$, 0.01, 0.001, respectively.

695

Table 4. Soil chemical properties before planting and after harvest

	Treatment	pH(H_2O)	Total amount of elements in soil (g pot^{-1})					
			Total carbon	Available Si	Exchangeable Ca	Exchangeable Mg	Exchangeable K	Exchangeable Na
before planting	B0	6.08 ± 0.02 b	219 ± 1 a	0.45 ± 0.01 ab	36.80 ± 0.35 ab	4.10 ± 0.05 a	4.74 ± 0.22 a	0.36 ± 0.06 bc
	B5	6.11 ± 0.03 b	225 ± 2 a	0.43 ± 0.01 b	36.28 ± 0.63 b	4.19 ± 0.05 a	4.56 ± 0.20 a	0.33 ± 0.02 c
	B10	6.12 ± 0.03 b	223 ± 3 a	0.43 ± 0.01 b	37.11 ± 0.38 ab	4.16 ± 0.02 a	4.59 ± 0.07 a	0.43 ± 0.08 bc
	B20	6.11 ± 0.00 b	223 ± 3 a	0.44 ± 0.01 b	36.71 ± 0.77 b	4.15 ± 0.07 a	5.31 ± 0.64 a	0.45 ± 0.05 bc
	B50	6.21 ± 0.01 a	230 ± 2 a	0.48 ± 0.01 ab	37.06 ± 0.38 ab	4.17 ± 0.05 a	4.94 ± 0.47 a	0.58 ± 0.02 b
	B100	6.26 ± 0.01 a	220 ± 2 a	0.50 ± 0.01 a	38.96 ± 0.36 a	4.32 ± 0.05 a	4.79 ± 0.19 a	0.94 ± 0.05 a
	ANOVA	***	**n.s.**	**	*	**n.s.**	**n.s.**	***
after harvest	B0	6.52 ± 0.11 a	226 ± 1 a	0.39 ± 0.01 c	43.59 ± 0.40 a	6.30 ± 0.05 c	2.02 ± 0.11 a	1.71 ± 0.11 b
	B5	6.54 ± 0.11 a	225 ± 6 a	0.37 ± 0.01 c	43.81 ± 1.22 a	6.60 ± 0.23 bc	1.97 ± 0.11 a	2.03 ± 0.17 b
	B10	6.66 ± 0.09 a	218 ± 5 a	0.41 ± 0.01 bc	44.31 ± 0.90 a	6.76 ± 0.12 abc	2.10 ± 0.08 a	1.76 ± 0.11 b
	B20	6.60 ± 0.09 a	227 ± 3 a	0.41 ± 0.01 bc	43.93 ± 0.32 a	6.58 ± 0.08 bc	1.99 ± 0.06 a	2.01 ± 0.08 b
	B50	6.67 ± 0.08 a	222 ± 2 a	0.43 ± 0.01 ab	44.40 ± 0.38 a	6.94 ± 0.11 ab	2.09 ± 0.09 a	2.23 ± 0.11 ab
	B100	6.64 ± 0.20 a	230 ± 3 a	0.47 ± 0.01 a	46.06 ± 1.18 a	7.30 ± 0.13 a	1.94 ± 0.14 a	2.74 ± 0.12 a
	ANOVA	**n.s.**	**n.s.**	***	**n.s.**	**	**n.s.**	***

Mean values ± one standard error are shown. Sample size before planting was three, while after harvest was four. “ANOVA” shows the results of one-way ANOVA, which was performed for detecting the significant differences among the treatments. Asterisks (*,**,***) denote $p < 0.05$, 0.01, 0.001, respectively. “n.s.” denotes not significant ($p > 0.05$). Different letters indicate significant differences among the treatments determined via

Tukey post hoc test. Each pot contained 8 kg of soil and basalt was additionally applied depending on the treatment of application rate.

Table 5. Dry weight of each part of rice at harvest

Treatment	Dry weight (g plant^{-1})					
	root	stem	leaf	husk	grain	total
B0	4.43 ± 0.29 a	47.0 ± 1.8 a	15.0 ± 0.1 a	21.3 ± 0.3 a	80.5 ± 1.8 a	168 ± 3.6 a
B5	4.87 ± 0.77 a	48.0 ± 2.3 a	15.7 ± 1.1 a	20.0 ± 0.6 a	74.1 ± 2.7 a	163 ± 7.1 a
B10	4.94 ± 0.42 a	51.3 ± 0.9 a	15.8 ± 0.9 a	22.1 ± 0.9 a	81.3 ± 3.2 a	175 ± 4.4 a
B20	5.90 ± 0.82 a	52.0 ± 2.7 a	14.7 ± 0.4 a	21.1 ± 0.1 a	76.8 ± 2.6 a	170 ± 5.5 a
B50	6.23 ± 0.62 a	52.3 ± 1.1 a	16.2 ± 0.7 a	21.2 ± 0.4 a	77.6 ± 1.0 a	174 ± 1.8 a
B100	5.64 ± 0.31 a	51.5 ± 1.5 a	17.4 ± 0.8 a	22.2 ± 0.5 a	80.7 ± 1.8 a	177 ± 4.3 a
ANOVA	**n.s.**	**n.s.**	**n.s.**	**n.s.**	**n.s.**	**n.s.**

Mean values ± one standard error are shown (n=4). “ANOVA” shows the results of one-way ANOVA, which was performed for detecting the significant differences among the treatments. “n.s.” denotes not significant ($p > 0.05$). No significant difference among the treatments was determined via Tukey post hoc test.

Table 6. Total uptake of elements in rice

Treatment	Total uptake of elements in rice (mg plant^{-1})											
	Si		Ca		Mg		K		Na			
B0	3603 ± 62	ab	284 ± 5	a	402 ± 7	a	2412 ± 106	a	126 ± 15	b		
B5	3539 ± 147	b	273 ± 18	a	376 ± 10	a	2430 ± 69	a	110 ± 10	b		
B10	3736 ± 50	ab	288 ± 16	a	410 ± 7	a	2437 ± 53	a	132 ± 7	b		
B20	3615 ± 163	ab	293 ± 20	a	390 ± 8	a	2447 ± 68	a	138 ± 4	b		
B50	3859 ± 45	ab	285 ± 17	a	388 ± 8	a	2349 ± 44	a	154 ± 17	ab		
B100	3959 ± 60	a	285 ± 9	a	402 ± 6	a	2468 ± 68	a	201 ± 17	a		
ANOVA	*****		**n.s.**		**n.s.**		**n.s.**		******			

Mean values ± one standard error are shown (n=4). “ANOVA” shows the results of one-way ANOVA, which was performed for detecting the significant differences among the treatments. Asterisks (*,**) denote $p < 0.05$, 0.01, respectively. “n.s.” denotes not significant ($p > 0.05$). Different letters indicate significant differences among the treatments determined via Tukey post hoc test.

712 **Table 7.** Concentrations of As and heavy metals in grain of rice

Treatment	Element concentration in grain (μg g^{-1} grain)					
	As	Cd	Cu	Cr	Ni	
B0	0.646 ± 0.017 a	0.0066 ± 0.0005 a	4.75 ± 0.04 a	1.88 ± 0.14 a	0.159 ± 0.013 a	
B5	0.654 ± 0.071 a	0.0100 ± 0.0021 a	5.40 ± 0.32 a	2.19 ± 0.27 a	0.177 ± 0.018 a	
B10	0.723 ± 0.045 a	0.0075 ± 0.0008 a	4.93 ± 0.10 a	1.85 ± 0.10 a	0.224 ± 0.037 a	
B20	0.691 ± 0.035 a	0.0080 ± 0.0008 a	4.67 ± 0.09 a	1.84 ± 0.11 a	0.138 ± 0.012 a	
B50	0.743 ± 0.061 a	0.0078 ± 0.0008 a	4.75 ± 0.46 a	2.66 ± 0.10 a	0.200 ± 0.036 a	
B100	0.746 ± 0.033 a	0.0079 ± 0.0018 a	4.97 ± 0.24 a	2.08 ± 0.29 a	0.142 ± 0.014 a	
ANOVA	**n.s.**	**n.s.**	**n.s.**	**n.s.**	**n.s.**	

713 Mean values ± one standard error are shown (n=4). “ANOVA” shows the results of one-way ANOVA, which was performed for detecting the
714 significant differences among the treatments. “n.s.” denotes not significant ($p > 0.05$). No significant difference among the treatments was
715 determined via Tukey post hoc test.

716

Table 8. Carbon balance between before planting and after harvest in the soil and in the whole system

Treatment	Carbon balance in the soil (gC pot^{-1})	Total amount of carbon in plant (gC pot^{-1})	Carbon balance in the whole system (gC pot^{-1})
B0	7.1 ± 1.4 a	69.6 ± 2.1 a	76.7 ± 3.2 a
B5	-0.1 ± 5.7 a	67.2 ± 3.0 a	67.1 ± 8.0 a
B10	-4.9 ± 5.4 a	72.4 ± 1.8 a	67.5 ± 6.9 a
B20	6.4 ± 2.0 a	70.4 ± 2.3 a	76.9 ± 4.3 a
B50	-7.3 ± 2.5 a	71.7 ± 0.7 a	64.4 ± 2.7 a
B100	10.1 ± 3.4 a	73.3 ± 1.8 a	83.4 ± 4.6 a
ANOVA	*****	**n.s.**	**n.s.**

Mean values ± one standard error are shown (n=4). “ANOVA” shows the results of one-way ANOVA, which was performed for detecting the significant differences among the treatments. Asterisk (*) denotes $p < 0.05$. “n.s.” denotes not significant ($p > 0.05$). No significant difference among the treatments was determined via Tukey post hoc test.

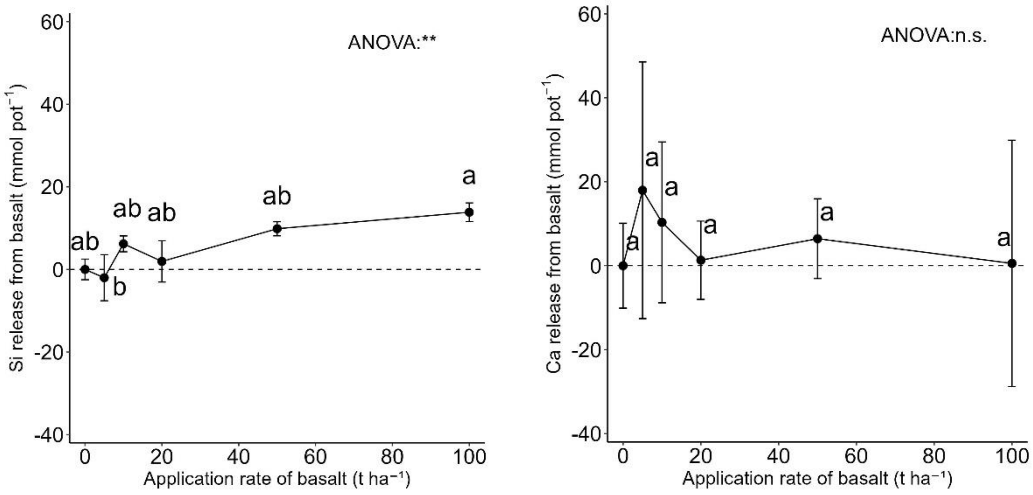
722

723

(a)

(b)

724

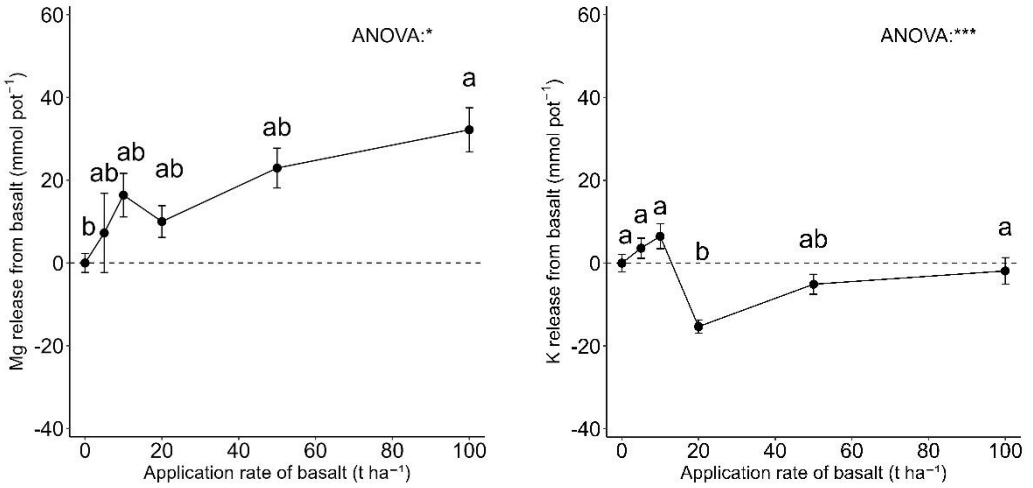


725

726

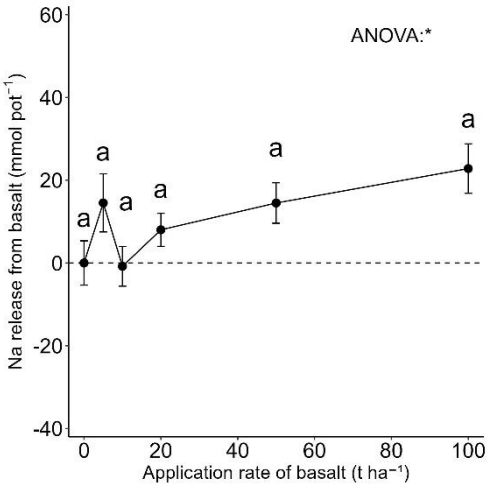
(c)

(d)



727

(e)



728

729

730 **Figure 1**. Release of Si **(a)**, Ca **(b)**, Mg **(c)**, K **(d)**, and Na **(e)** from basalt during cultivation.
731 Points represent mean values ± one standard error (n=4). "ANOVA" shows the results of one-
732 way ANOVA, which was performed to detect the significant differences among the application
733 rates of basalt. Asterisks (*,**,***) denotes $p < 0.05$, 0.01, 0.001, respectively. "n.s." denotes
734 not significant ($p > 0.05$). Different letters indicate significant differences among the application
735 rates of basalt determined via Tukey post hoc test.

736

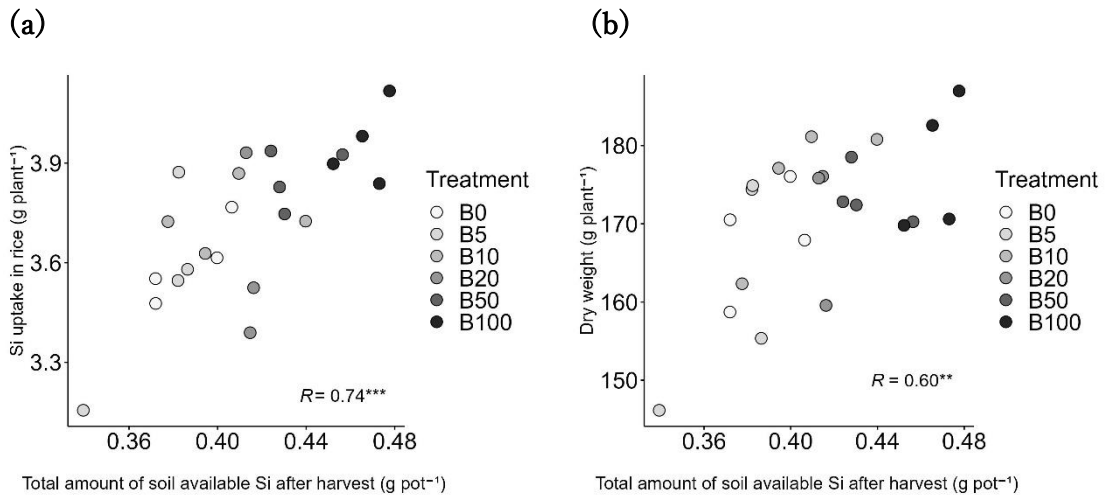


Figure 2. Relationship between total amount of soil available Si after harvest and Si uptake in rice **(a)** and total dry weight **(b)**. **(a)** Points represents values of each sample. Linear regression analysis was performed. *R* denotes the Pearson product moment correlation coefficient. Asterisks (***) denotes $p < 0.001$. **(b)** Points represents values of each sample. Linear regression analysis was performed. *R* denotes the Pearson product moment correlation coefficient. Asterisks (**) denotes $p < 0.01$.

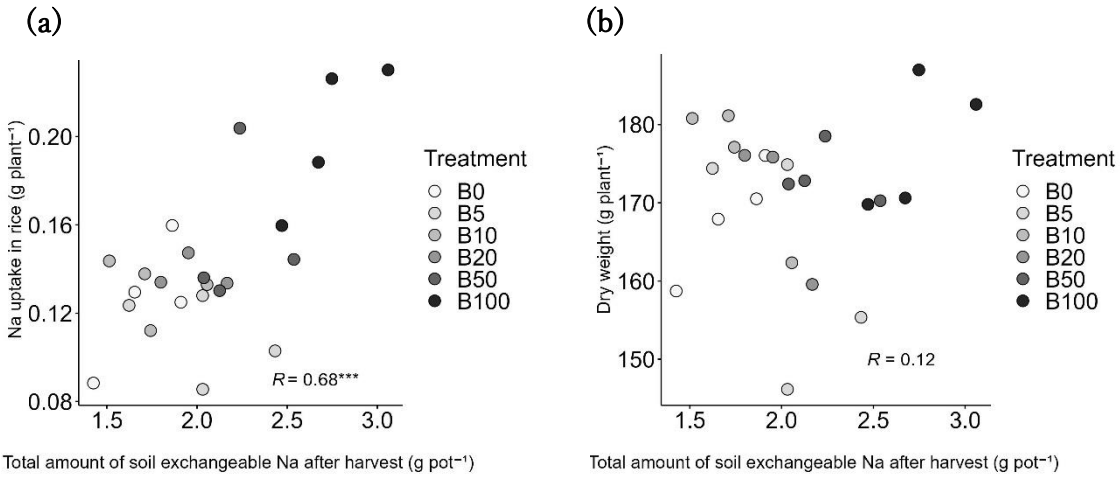
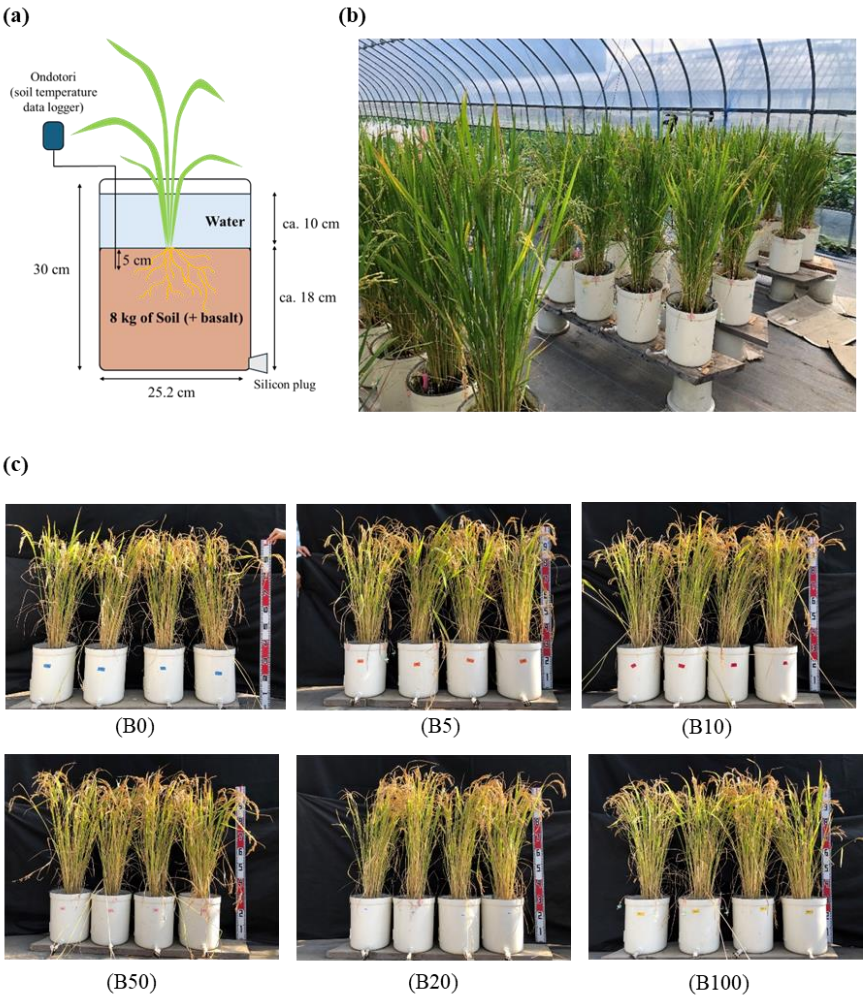


Figure 3. Relationship between total amount of soil exchangeable Na after harvest and Na uptake in rice **(a)** and total dry weight **(b)**. **(a)**Points represents values of each sample. Linear regression analysis was performed. *R* denotes the Pearson product moment correlation coefficient. Asterisks (***) denotes $p < 0.001$. **(b)**Points represents values of each sample. Linear regression analysis was performed. *R* denotes the Pearson product moment correlation coefficient. No significance was observed ($p > 0.05$).



Supplemental figure 1. Schematic diagram of the pot **(a)** and photograph of status of the experiment on 20th August 2022 (2 months in) **(b)** and on 22nd September (at harvest) **(c)**.

Supplemental table 1. Element concentration in the soil

	Basalt	Total carbon	Element concentration in soil (mg kg⁻¹ soil)				
	(t ha⁻¹)	(g kg^{-1} soil)	Available Si	Exchangeable Ca	Exchangeable Mg	Exchangeable K	Exchangeable Na
before planting	B0	27.4 ± 1.5 a	56.8 ± 1.0 a	4600 ± 44 a	512 ± 6 a	592 ± 27 a	45 ± 8 b
	B5	28.1 ± 2.2 a	53.8 ± 1.7 a	4521 ± 79 a	522 ± 7 a	569 ± 25 a	41 ± 2 b
	B10	27.7 ± 4.2 a	53.6 ± 1.6 a	4610 ± 47 a	517 ± 2 a	570 ± 8 a	54 ± 10 b
	B20	27.5 ± 3.2 a	54.2 ± 1.4 a	4532 ± 96 a	512 ± 8 a	655 ± 79 a	56 ± 6 b
	B50	27.8 ± 2.7 a	58.3 ± 1.7 a	4492 ± 47 a	505 ± 6 a	599 ± 57 a	70 ± 3 b
	B100	25.8 ± 2.0 b	58.9 ± 1.6 a	4584 ± 42 a	508 ± 6 a	563 ± 23 a	111 ± 6 a
	ANOVA	**	**n.s.**	**n.s.**	**n.s.**	**n.s.**	***
after harvest	B0	28.3 ± 1.7 a	48.4 ± 1.1 bc	5449 ± 50 a	788 ± 6 a	253 ± 14 a	214 ± 14 b
	B5	28.1 ± 7.1 a	46.4 ± 1.4 c	5459 ± 152 a	822 ± 29 a	246 ± 13 a	253 ± 21 b
	B10	27.1 ± 6.7 a	50.3 ± 1.6 abc	5504 ± 111 a	839 ± 15 a	261 ± 10 a	218 ± 14 b
	B20	28.0 ± 3.3 a	50.0 ± 1.2 abc	5423 ± 39 a	812 ± 10 a	246 ± 8 a	248 ± 10 b
	B50	27.0 ± 3.0 a	52.7 ± 0.9 ab	5381 ± 46 a	841 ± 13 a	253 ± 11 a	271 ± 13 ab
	B100	27.0 ± 3.9 a	54.9 ± 0.7 a	5419 ± 138 a	859 ± 15 a	228 ± 17 a	322 ± 14 a
	ANOVA	**n.s.**	**	**n.s.**	**n.s.**	**n.s.**	***

Mean values ± one standard error are shown. Sample size before planting was three, while after harvest was four. "ANOVA" shows the results of one-way ANOVA, which was performed for detecting the significant differences among the application rate of basalt. Asterisks (*,**,***) denote *p*

762 < 0.05, 0.01, 0.001, respectively. “n.s.” denotes not significant ($p > 0.05$). Different letters indicate significant differences among the treatments
763 determined via Tukey post hoc test.

764

765 **Supplemental table 2.** Yield-related indices of rice

Treatment	panicle number ($plant^{-1}$)	grain number ($panicle^{-1}$)	1000 grain weight (g)	setting rate (%)
B0	58.3 ± 1.0 a	65.4 ± 1.9 a	22.4 ± 0.1 a	0.889 ± 0.039 a
B5	55.8 ± 1.1 a	66.0 ± 2.7 a	22.7 ± 0.3 a	0.892 ± 0.041 a
B10	60.3 ± 2.1 a	65.3 ± 4.5 a	22.4 ± 0.2 a	0.927 ± 0.011 a
B20	55.0 ± 1.5 a	68.4 ± 1.9 a	22.4 ± 0.4 a	0.914 ± 0.009 a
B50	59.5 ± 2.1 a	64.9 ± 3.0 a	22.7 ± 0.1 a	0.891 ± 0.024 a
B100	61.0 ± 2.9 a	65.0 ± 1.9 a	22.3 ± 0.2 a	0.918 ± 0.011 a
ANOVA	**n.s.**	**n.s.**	**n.s.**	**n.s.**

766 Mean values ± one standard error are shown (n=4). "ANOVA" shows the results of one-way ANOVA, which was performed for detecting the
767 significant differences among the application rate of basalt. "n.s." denotes not significant ($p > 0.05$). No significant difference among the treatments
768 was determined via Tukey post hoc test.

769

770

771 **Supplemental table 3.** Release rate of Si, Ca, Mg, K, and Na from the basalt

Source	Basalt application rate		Release rate (mmol m^{-2} day^{-1})				
	(t ha^{-1})	(wt. %)	Si	Ca	Mg	K	Na
This study	0	0	0.0 ± 0.5	0.0 ± 2.0	0.0 ± 0.5	0.0 ± 0.4	0.0 ± 1.1
	5	0.31	-0.4 ± 1.1	3.6 ± 6.2	1.5 ± 1.9	0.7 ± 0.5	2.9 ± 1.4
	10	0.63	1.3 ± 0.4	2.1 ± 3.9	3.3 ± 1.1	1.3 ± 0.6	-0.2 ± 1.0
	20	1.25	0.4 ± 1.2	0.3 ± 2.2	2.0 ± 0.9	-3.1 ± 0.4	1.6 ± 0.9
	50	3.13	2.0 ± 0.3	1.3 ± 1.9	4.6 ± 1.0	-1.0 ± 0.6	2.9 ± 1.0
	100	6.25	2.8 ± 0.5	0.1 ± 5.9	6.5 ± 1.1	0.4 ± 0.6	4.6 ± 1.2
Kelland et al. (2020)	100	3.63	1.9 ± 0.4	18 ± 14	4.2 ± 0.9	1.1 ± 1.4	0.33 ± 0.53

772 Mean values ± one standard error are shown (n=4). “wt. %” means the proportion of applied basalt powder to soil mixed with by weight. The surface
773 area of the pot was 0.05 m^{-2} and the cultivation duration was 99 days.

774